

RESEARCH

Open Access

Biogeochemistry and ecology of *Pyrosoma spinosum* from the Central Arabian Sea

Mangesh Gauns*, Sunita Mochemadkar, Anil Pratihary, Rajdeep Roy and Syed Wajih Ahmad Naqvi

Abstract

Background: A swarm of pelagic tunicate (*Pyrosoma spinosum*) was found in the surface open waters of the Arabian Sea during late southwest monsoon (September 2007). The swarm site was characterized by moderate southwesterly wind (approximately 7 m s^{-1}), relatively low sea-surface temperature (approximately 26°C), shallow mixed layer (approximately 50 m), and substantial macro-nutrient concentrations (surface values: $2.5 \mu\text{M}$ nitrate, $0.3 \mu\text{M}$ phosphate, $0.9 \mu\text{M}$ silicate, and $5.0 \mu\text{M}$ ammonium). Despite adequate macronutrient availability, the swarm site was characterized by low diversity of phytoplankton ($>5 \mu\text{m}$) and mesozooplankton in the upper 200 m. Low chlorophyll *a* concentration (27.3 mg/m^2 in the upper 120 m) at the swarm site was dominated (90% to 95% in the upper 40 m) by the *Synechococcus* ($20 \times 10^6 /\text{ml}$).

Results: Silicate deficiency in surface waters upwelled or entrained from the thermocline may be a key factor for the dominance of smaller autotrophs (flagellates and cyanobacteria) that seems to offer favorable conditions for episodic occurrence of swarms of these filter feeders. Low carbon content (37% of total dry weight) and the lower molar (carbon-to-nitrogen) ratio (5) in *P. spinosum* suggest growth of these organisms is carbon-limited.

Conclusions: We describe various physicochemical and biological conditions at the *P. spinosum* swarm location and at two other nearby sites not affected by it. The biological factors predominantly high densities of *Synechococcus* and flagellates were best suited conditions for the proliferation of pyrosome biomass in the central Arabian Sea.

Keywords: *Pyrosoma spinosum*; Arabian Sea; Biogeochemistry; Phytoplankton; Zooplankton

Background

Pyrosoma is a genus of warm-water protochordates consisting of a large number of small individual organisms (called zooids), which remain together in the form of a drifting colony. These colonies range in size from microscopic to $>10 \text{ m}$ long (Griffin and Yaldwyn 1970). Interestingly, each zooid of the colony remains independent of others. Each zooid feeds by passing a current, containing particles and organisms, through a mucus-covered branchial basket that retains particles including bacteria. Picophytoplanktons, which contribute significantly to the global primary production, are abundantly found in the Arabian Sea even during the southwest monsoon period (Brown et al. 1999). Analysis of gut contents of *Pyrosoma* (Hart, as cited by Culkin and Morris 1970) showed that the main food (80%) was phytoplankton belonging to the classes Haptophyceae, Chrysophyceae, and

Bacillariophyceae. The remainder was composed of protozoan species such as radiolarians and tintinnids.

Geographically, pyrosome forms are found distributed worldwide, commonly in the warm tropical and temperate waters, particularly between 50°N and 50°S (Sewell 1953, Van Soest 1981) but not in polar waters. In the water column, they occur at the surface as well as in the dark region of the deep sea. They have been collected from depths well in excess of 3,000 m (Millar 1971).

The trophodynamic role of other pelagic tunicates such as salps, doliolids, and appendicularians in the pelagic ecosystem is known to some extent (see Harbison and Gilmer 1976, Wiebe et al. 1979, Alldredge 1981, Deibel 1982, 1986, 1988, Madin 1982, Madin and Cetta 1984, Naqvi et al. 2002). In comparison, much less is known about pyrosomes even though early work on these tunicates dates back to early nineteenth century (Peron 1804). The pyrosomes as pelagic zooplankton are of special interest in the trophodynamics of planktonic ecosystems as they occasionally rival crustaceans as the dominant planktonic

* Correspondence: gmangesh@nio.org
National Institute of Oceanography (Council of Scientific and Industrial Research), Dona Paula, Goa 403004, India

herbivores (Thompson 1948, Bary 1960). The presence of these forms considerably increases the standing crop of secondary producers (Angel 1989). That study also points out that pyrosomes undertake extensive vertical migration going down to 500 to 700 m or even deeper during the day and ascending into the mixed layer at night. The vertical movement of these organisms highlights the importance of biological factors influencing the fluxes of material (Roe et al. 1987), similar to myctophids (Morrison et al. 1999) and copepods (Wishner et al. 2008, Takahashi et al. 2009).

The only mention of *P. spinosum* (apart from *P. verticillatum*, *P. aberniosum*, and *P. atlanticum*) comes from the southern part of the Arabian Sea (off the Arabian coast and in the Gulf of Aden) during the John Murray Expedition (1933 to 1934) (Sewell 1953) and from the work of Neumann (1913) from the equatorial zone (8°N to 10°S). During the IOE (1960 to 1965), pyrosomes were found restricted to the south of 10°N (see Indian Ocean Biological Centre 1973). However, occurrence of massive pyrosome colonies is at least not known in the northern Arabian Sea. This article records their occurrence in the region based on observations made in the summer of 2007. The possible reason and significance are examined in the present study.

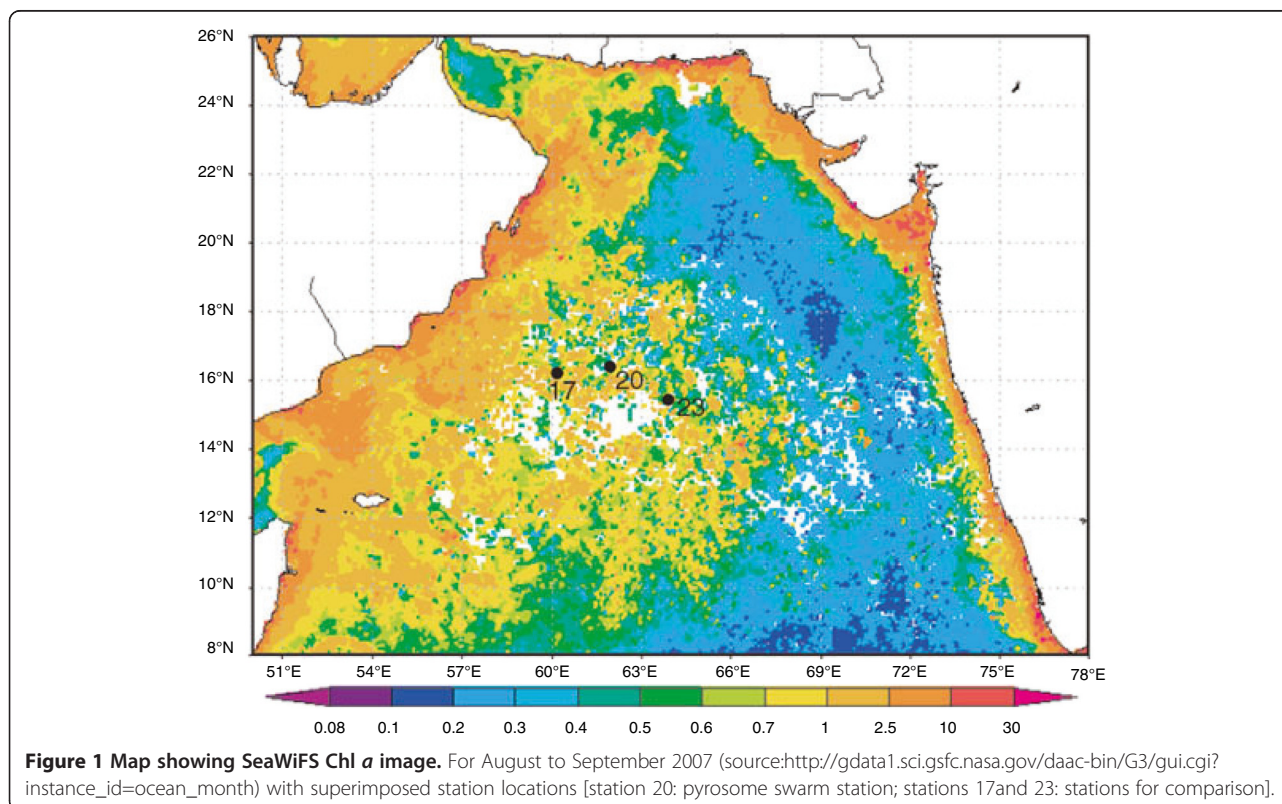
Methods

The climate and oceanographic processes of the Arabian Sea, our study area, is very different from the other

ocean basins as a result of its uncommon geographical setting. This region experiences seasonally reversing monsoon winds. The winds blow from the northeast in winter (November to February; northeast monsoon) and from the southwest in summer (June to September; southwest monsoon). The southwest monsoon is the most important period for the region because the strong southwesterly wind forces vigorous upwelling off Somalia, Yemen, and Oman in the western Arabian Sea are resulting in large-scale nutrient enrichment of the euphotic zone that extends about 1,000 km offshore. The present study was carried out to the end of the southwest monsoon in 2007.

Sampling

During the middle of the day, a pyrosome swarm was observed during a cruise of R/V *Roger Revelle* cruise at station 20 (lat. 15° 58' N; long. 62° 00' E; Figure 1) on 10 September 2007. The pyrosome colonies appeared to be long, pinkish-red colored, worm-like floating objects due to water motion. Specimens were collected without causing much damage with a large capacity (20 L) wide-mouth plastic bucket. The longest colony was roughly 0.8 m long and 16 cm wide; since it was cut and open on one side, the actual length must have been even longer. A much longer colony (approximately 2 m) was recovered at night entangled to the CTD rosette (cast to



120 m; see Additional file 1). Tubular colonies were cut open to measure the length and width.

To explore the ecological and biogeochemical significance of pyrosome swarm, we collected physicochemical and biological data from the swarm station as well as from two other nearby stations that were occupied on 9 September 2007 (station 17: lat. 15° 47.77'N, long. 60° 15.02'E) and on 12 September 2007 (station 23: lat. 15° 00'N, long. 63°59'E). All three stations were sampled during the day. Water samples were collected and processed as per JGOFS Protocols (UNESCO 1994). Temperature and salinity profiles were obtained from a conductivity-temperature-depth (CTD) unit (Sea Bird Electronics, Bellevue, WA, USA) mounted on a rosette having 24, 12-liter Go-FLO bottles (General Oceanics, Miami, FL, USA) for water sampling. Water samples were collected from different depths in the upper 120 m for chemical measurements and for estimating phytoplankton composition and standing stock (total- and size-based chlorophyll *a*), enumeration of heterotrophic nanoflagellates and bacteria. Mesozooplankton samples were collected from five strata (based on the physical structure of the water column) using a Multiple Plankton Net (200 μ m; HYDRO-BIOS, Kiel-Holtenau, Germany) from the upper 1,000 m. Details of sampling and processing procedures are as follows.

Chemical measurements

Chemical analyses of water samples for dissolved oxygen and nutrients were performed following standard procedures (SCOR 1996). Dissolved oxygen was analyzed following the Winkler titrimetric procedure using an automated system built and supplied by the Scripps Institution of Oceanography/Ocean Data Facility (SIO/ODF) group. Nutrients were measured with a SKALAR Analyzer (SKALAR, Breda, the Netherlands).

A portion of the colony was frozen at -80°C , and the remainder was then preserved separately in ethanol (70%) and hexamine-buffered formaldehyde (4%). Small portions of the colony (3×3 cm, approximately 60 zooids) were thoroughly washed in milli-Q water (Millipore Corporation, Darmstadt, Germany) and dried at 60°C for measurements of C-to-N ratio and stable isotopic ($\delta^{13}\text{C}$ and $\delta^{15}\text{N}$) composition by an isotopic ratio mass spectrophotometer coupled to an elemental analyzer. Isotopic ratios were measured relative to Peedee Belemnite for carbon and atmospheric N_2 for nitrogen. Precision values of 0.2‰ for $\delta^{13}\text{C}$ and 0.3‰ for $\delta^{15}\text{N}$ were obtained by multiple measurements of an external standard. Protein content of the organism extracted using the method of Rausch (1981) was quantified following Bradford (1976). For this purpose, two randomly picked pieces of the *Pyrosoma* colony (3×3 cm) were freeze-dried before extraction in 5 ml

of buffer (in triplicate). Absorbance was measured at 595 nm.

Biological measurements

Phytoplankton biomass (chlorophyll *a*)

Duplicate samples (1 L) from each depth (0, 10, 20, 40, 60, 80, 100, and 120 m) were filtered through 47-mm GF/F filters (0.7 μ m pore size). Chlorophyll *a* (Chl *a*) was extracted in 10 ml of 90% acetone in the dark for 24 h at 4°C . A fluorometer (Turner Designs, Sunnyvale, CA, USA) was used for measuring fluorescence.

Size-fractionated phytoplankton biomass

A known volume of water sample (2 to 5 L) was passed serially through different pore size filters (200, 60, 20, and 10 μ m nylon and 0.7 μ m GF/F). These filters were then processed following the procedure described above for total Chl *a*.

Phytoplankton cell counts ($>10 \mu\text{m}$)

A sub-sample of 250 ml from each of the above mentioned eight depths was fixed in 2% Lugol's iodine and preserved by adding 3% formaldehyde. All samples were stored in the dark at room temperature until enumeration. A settling and siphoning procedure was followed to concentrate the samples. Two replicates of 1 mL of the concentrated samples were then examined microscopically in a Sedgewick-Rafter plankton counting chamber (Structure Probe, Inc., West Chester, PA, USA) at $\times 200$ magnification.

Flow cytometry

Abundances of *Synechococcus* and picoeukaryotes were determined in glutaraldehyde (1% final concentration) fixed samples. All samples were frozen instantly in liquid nitrogen. Population was identified on FACSCalibur (Becton-Dickinson Biosciences, Franklin Lakes, NJ, USA) flow cytometer according to population fluorescence and light scatter characteristics (Vaulot et al. 1990).

HPLC pigments

Water samples (2 to 3 L) for pigment analyses were filtered through GF/F (0.7 μ m, 25 mm diameter) and the filters stored at -85°C until analysis in the shore laboratory a few weeks after the cruise. Phytoplankton pigments from the frozen filters were extracted in 3 ml 95% acetone (v/v in deionized water) in 5 min, using an ultrasonic bath (5 s, 20 kHz) filled with ice water. These extracts were then stored overnight at -20°C for high performance liquid chromatography (HPLC) analysis. Samples were later passed through a Teflon syringe cartridge (Millipore) (pore size 0.45 μ m, diameter 25 mm) to remove the cellular debris. The clear extract was collected in a 2-ml glass vial and placed directly into the

temperature-controlled (5°C) auto-sampler tray for HPLC analysis. The entire extraction procedure was carried out in dim light conditions and at low temperature to minimize degradation of pigments. The HPLC analysis was carried out following the method of Van Heuvel (2002) as detailed in Roy et al. (2006); however, the buffer used in this case was Tetrabutylammonium Acetate which had a concentration of 0.025 M. In the present study, the sum of 19-hexanoyloxyfucoxanthin (19'HF), 19-butanoyloxyfucoxanthin (19BF), alloxanthin (Allo), and chlorophyll *b* was used to indicate nanoflagellate abundance. Zeaxanthin (Zea), fucoxanthin (Fuc), and peridinin (Per) were considered to represent cyanobacteria, diatoms, and dinoflagellates, respectively. Diagnostic pigment (DP) indices were calculated following the method of Barlow et al. (2007) for assessing the phytoplankton communities. Four major groups were evaluated. The indices representing the groups were designated as $Diat_{DP}$ (diatoms), $Dino_{DP}$ (dinoflagellates), $Flag_{DP}$ (nanoflagellates), and $Prok_{DP}$ (Prokaryotes).

Bacterial abundance

Sub-samples (20 to 50 ml) from each of the depths mentioned above and additionally from 150, 200, 300, 500, 600, and 800 m were fixed with 4% of 0.22- μ m-filtered formaldehyde and stored at 4°C until DAPI stained direct counts (AODC) were made. Counting was done using an Olympus BH2 epifluorescence microscope (Olympus Corp., Tokyo, Japan).

Heterotrophic nanoflagellates

In order to determine the abundance of heterotrophic nanoflagellates, 100 ml of each water sample was fixed in glutaraldehyde (2% final concentration). A known volume of water was filtered through 0.8 μ m black Nuclepore (Nuclepore, NJ, USA) filters (Booth 1993) after staining with DAPI and proflavine at the final concentration of 5 μ g/ml and allowing staining for 5 min (Hass 1982, Booth 1993). Slides were prepared and held at 5°C in a darkened box until used for epifluorescence microscopy.

Mesozooplankton biomass (ZP)

The biomass of mesozooplankton was estimated as displacement volume after blotting it on an absorbent paper and then measuring in a graduated cylinder. This was done before preservation of the sample. In the shore laboratory, organisms were identified to the genus (species level in some forms) level under a stereo zoom microscope (magnification \times 160; Nikon Corp., Tokyo, Japan).

Results

Physico-chemical parameters

The *P. spinosum* swarm was found at station 20. This region (study location) experienced relatively weaker

southwesterly winds (3.3 to 9.9 $m s^{-1}$; average 6.8 ± 1.5). Similarly, variations in air temperature were well within 1°C (25.5 to 26.1; average $25.8 \pm 0.15^\circ C$). Sea surface temperature (SST) at station 17 (located to the southwest of study location; Figure 1) was 0.5°C cooler than the other two stations (20 and 23) indicating a greater influence of upwelled water advecting offshore from the coastal upwelling sites. At the latter two stations, both temperature and salinity were also low (Figure 2A, B). The mixed layer depth (MLD, inferred from the temperature profiles) was shallower at stations 20 and 17 (approximately 50 m) than at station 23 (approximately 70 m; Figure 2A). However, despite the deeper MLD and more offshore location of station 23, surface nitrate concentration at this station was slightly higher (approximately 4 μ M) than at station 20 (approximately 2.5 μ M). Station 17 had much higher surface nitrate, approximately 11 μ M. A similar trend was observed with phosphate (Figure 3B) and silicate (Figure 3C), but ammonium was significantly higher (two- to sixfold) at station 20 (approximately 5 μ M) than at other two stations. Dissolved oxygen concentrations (Figure 4) were <0.5 ml/L between 200 and 1,000 m (except at 250 m) at station 20. Even lower concentrations (close to or below the detection limit between 150 and 500 m) were recorded at station 23.

Biological parameters

Chlorophyll a (total and size fractionated; fluorometric analysis)

Contrary to expectations, availability of substantial macronutrients in surface waters at all three stations did not result in commensurately high Chl concentrations. This is consistent with the results of Naqvi et al. (2010) who proposed that phytoplankton productivity in this region is limited by iron toward the end of the southwest monsoon. However, despite the lowest macronutrient levels in surface waters among the three stations, the phytoplankton biomass was the highest at station 20, for both the surface Chl *a* concentration (0.60 mg/m^3) and the column inventory (27.3 mg/m^2 ; 0 to 120 m). The total biomass (equivalent to station 17) was roughly 11.55 mg/m^2 higher than at station 23 (Figure 5A). Further, analysis of phytoplankton biomass in different size fractions, carried out by gravity filtration, showed higher biomass in the larger (>20 μ m) fractions (approximately 48%, Figure 5B) at stations 17 and 23 than at station 20, where the biomass were largely dominated by the smaller (<20 μ m) fractions, (approximately 79%; Figure 5B) indicating the dominance of pico- and nanoautotrophs. Further, the lower phaeopigment-to-chlorophyll ratio in the upper 60 m was significantly lower (0.3 ± 0.18) at station 20 than at the other two stations (0.5 ± 0.3) indicating relatively healthy autotrophic cells prevailing at station 20.

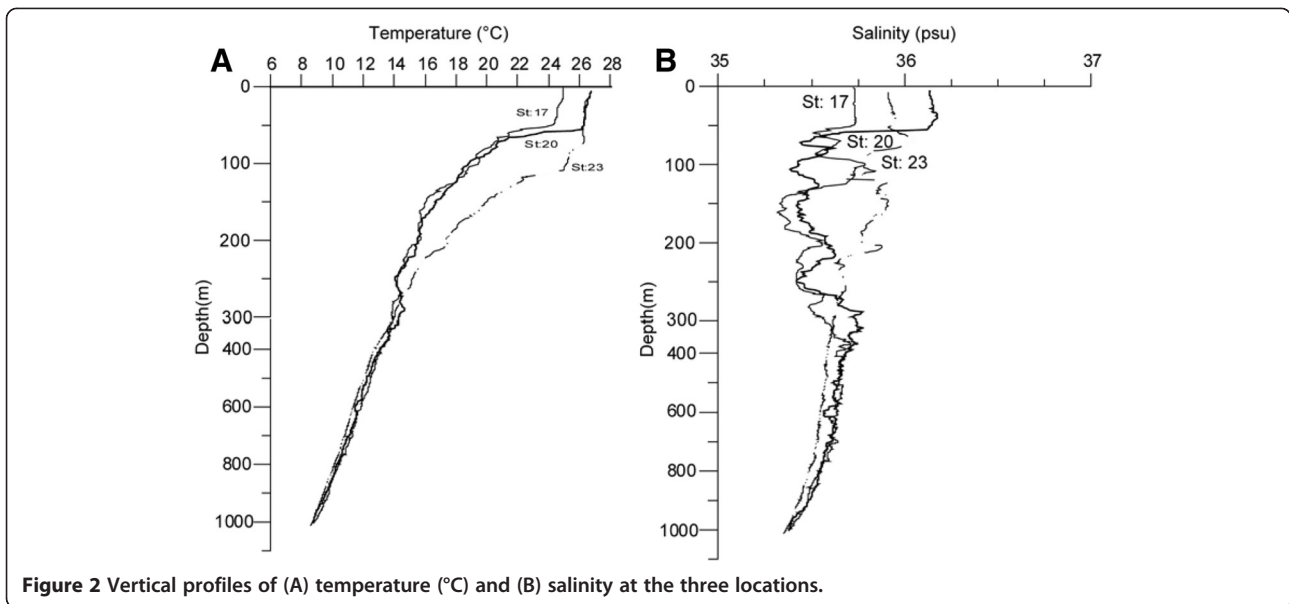


Figure 2 Vertical profiles of (A) temperature (°C) and (B) salinity at the three locations.

Phytoplankton cell abundance and composition (microscopic analyses of >10 μm cells)

Numerically averaged cell proportion of diatoms in the phytoplankton community excluding *Phaeocystis* was lower at station 20 (46%) than station 23 (74%) and 17 (94%; Figure 6A) indicating the overall dominance of diatoms at the two latter stations. It was interesting to find centric diatoms (chain forming in particular) dominating at station 20 (Table 1; Figure 6B, C). Further, dinoflagellate contribution at the swarm region (station 20) was the least (3%; Figure 6D). Overall, phytoplankton diversity was also low at station 20: altogether, 22, 15, and 18 genera were recorded at stations 23, 20, and 17, respectively (Table 1).

Phaeocystis distribution was patchy both geographically and vertically in the water column. They were found at surface (stations 17 and 23), 10 m (stations 20 and 23) and at 40 m (station 20). Maximum cell counts ($86 \times 10^6/L$) were found at 10 m of station 23 and the least at station 17 ($0.01 \times 10^6/L$). At station 20, *Phaeocystis* were found even at a deeper depth (40 m; $18.4 \times 10^6/L$). Their contribution to total phytoplankton abundance was sizable (see Figure 6A). At a few depths, their contribution to the total phytoplankton abundance was as high as 99.99%. A near-surface maximum of *Phaeocystis* (52% of the total phytoplankton abundance) was found only at station 17 (Figure 6A).

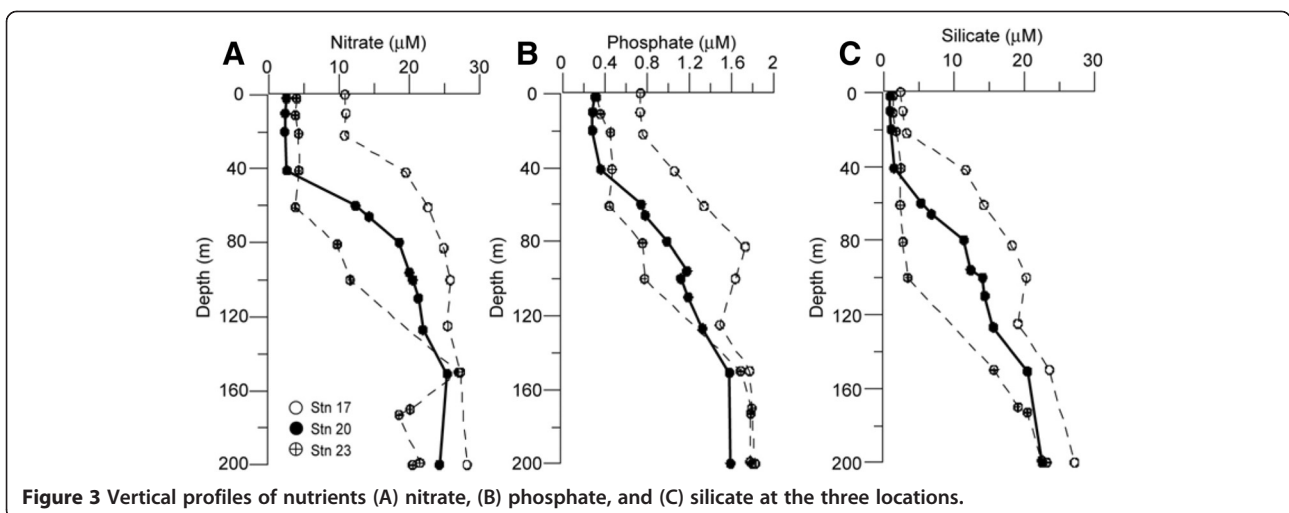


Figure 3 Vertical profiles of nutrients (A) nitrate, (B) phosphate, and (C) silicate at the three locations.

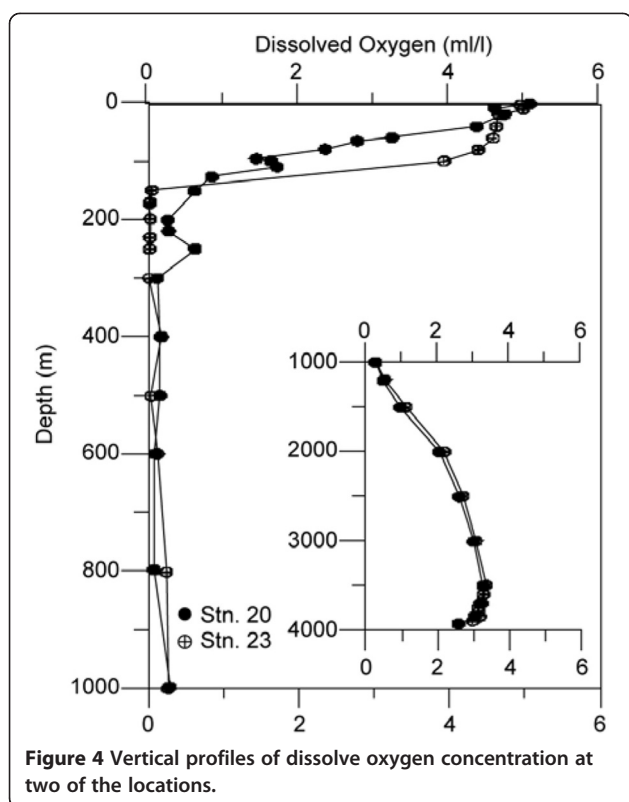


Figure 4 Vertical profiles of dissolve oxygen concentration at two of the locations.

Picophytoplankton (flow cytometry based)

Flow cytometric data yielded a *Synechococcus* count at station 20 (approximately $20 \times 10^6/\text{ml}$ at the surface) that was 2.5 and 9.5 times higher than the corresponding counts at stations 17 and 23, respectively (Figure 7A). Conversely, the number of picoeukaryotes were the least at station 20 ($0.12 \times 10^6/\text{ml}$), compared to the counts at the other sites of $0.15 \times 10^6/\text{ml}$ at station 17 and $0.27 \times 10^6/\text{ml}$ at station 23 (Figure 7B).

Pigment analyses (HPLC based)

Overall, phytoplankton pigments remained low, resembling nearly oligotrophic conditions. The pigment-derived diagnostic index (Figure 8), based on Barlow et al. (2007), revealed systematic differences in phytoplankton composition between stations (17, 20, and 23). Diat_{DP} proportion ranged from 0.04 to 0.16 at station 20 and from 0.12 to 0.19 at station 23, substantially lower than at station 17 (0.21 to 0.32). Dino_{DP} also showed a similar trend with minor increase below the surface at station 17. The Flag_{DP} proportion representing the nanoflagellates was substantially higher than those of the larger phytoplankton groups, ranging between 0.41 and 0.58. The Prok_{DP} proportion, used to denote zeaxanthin containing cyanobacteria, showed significant increases at Stations 20 (and 23) suggesting the dominance of

prokaryotes at these stations unlike station 17 where the Prok_{DP} was low. Based on the diagnostic index, the order of dominance of phytoplankton groups at stations 20 and 23 was $\text{Flag}_{\text{DP}} > \text{Prok}_{\text{DP}} > \text{Diat}_{\text{DP}} > \text{Dino}_{\text{DP}}$. At station 17, the order was $\text{Flag}_{\text{DP}} > \text{Diat}_{\text{DP}} > \text{Dino}_{\text{DP}} > \text{Prok}_{\text{DP}}$. Thus, flagellates appear to have been the most important autotrophs at all stations followed by cyanobacteria at stations 20 (and 23), and by diatoms at station 17.

Bacterial abundance

Bacterial abundance at station 20 (swarm site) was much lower as compared to non-swarm region even though in the upper water column their abundance showed a comparable vertical distribution at stations 20 and 23 (Figure 9A), except for an increase in abundance within the suboxic zone of station 23. Peak abundances found just below the surface (20 to 40 m) at station 17 was approximately threefold higher ($1.1 \times 10^9 /\text{L}$) than at stations 20 (and 23).

Heterotrophic nanoflagellates

Intriguingly, heterotrophic nanoflagellates (HNF) showed a trend different from that of bacterial abundance. In this case, abundance and depth profiles were similar for stations 17 and 23, but at station 20, a large increase in the HNF population occurred at 20 m depth ($0.17 \times 10^7/\text{L}$) with elevated numbers persisting down to at least 60 m. Similar to the bacterial population, little differences were observed below 80 m depth (Figure 9B). There was a significant correlation (Figure 9C) between heterotrophic nanoflagellates and bacteria ($p < 0.001$, $n = 40$), although the r^2 value was only 0.5.

Mesozooplankton

Mesozooplankton (>200 μm in size) abundance in the upper 1,000 m (0 to 200 m/200 to 1,000 m) did not differ much between stations 17 ($2,349/1,579 \text{ m}^{-3}$) and 20 ($2,378/1,057 \text{ m}^{-3}$). On the other hand, abundance at station 23 was nearly twofold higher ($4,670/736 \text{ m}^{-3}$), particularly in the upper layer. Biomass also showed a similar trend with twofold higher values at station 23 ($82 \text{ ml}/100\text{m}^3$; Table 1). Vertically, 88% to 97% of the biomass was in the upper 200 m (Figure 10A) particularly within the MLD. Overall, both numbers of organisms and their biomass decreased with increasing depth in the upper 1,000 m (Figure 10A).

Mesozooplankton composition in the region was dominated by 15 groups. Overall, diversity of these forms did vary between the stations. Most diverse forms belonged to copepoda family, such as *Calanidae*, *Paracalanidae*, *Euchaetidae*, *Scolecitrichidae*, *Centropagidae*, *Temoridae*, *Acartidae*, *Candaciidae*, *Pontellidae*, *Aetideidae*, *Heterorhabdidae*, *Lucicutidae*, *Augaptilidae*, *Monstrillidae*, *Mormonillidae*, and *Metridinidae*. Most abundant

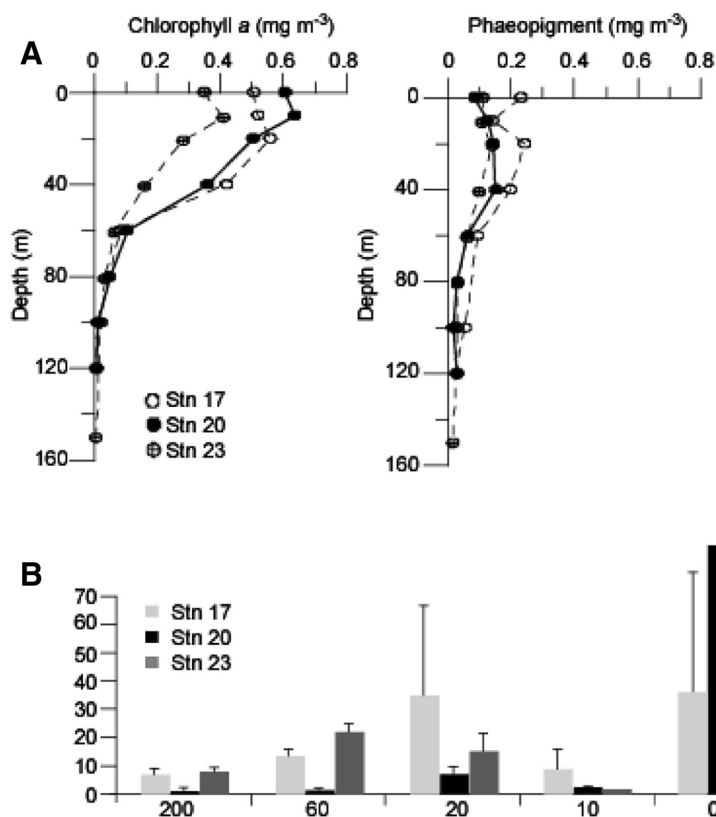


Figure 5 Vertical profiles of total and percent chlorophyll. (A) Total chlorophyll *a* and phaeopigments; (B) percent chlorophyll *a* biomass in different fractions (μm) at different locations.

copepods present were *Oncea* spp., *Corycaeus* spp., and *Paracalanus* spp. while few representatives belonging to *Cyclopoida*, *Poecilostomatoida*, and *Harpacticoida* were also found (Table 2).

The integrated biomass and abundance data in the upper 120 m are plotted in Figure 10B. Total Chl *a* biomass was relatively higher at stations 20 and 17 (average 27 mg/m²) compared to station 23 (15.6 mg/m²). In contrast, phytoplankton abundance of smaller forms (<10 μm) dominated by *Synechococcus* was higher at station 20. The significance of *Synechococcus* is confirmed by flow cytometric and HPLC data. Possibly, observed high population of heterotrophic nanoflagellates was responsible for sustaining lower bacterial counts through grazing at station 20 (and also at station 23). Further, average biomass and abundance of mesozooplankton at stations 20 (and 17) was twofold lower than that at station 23.

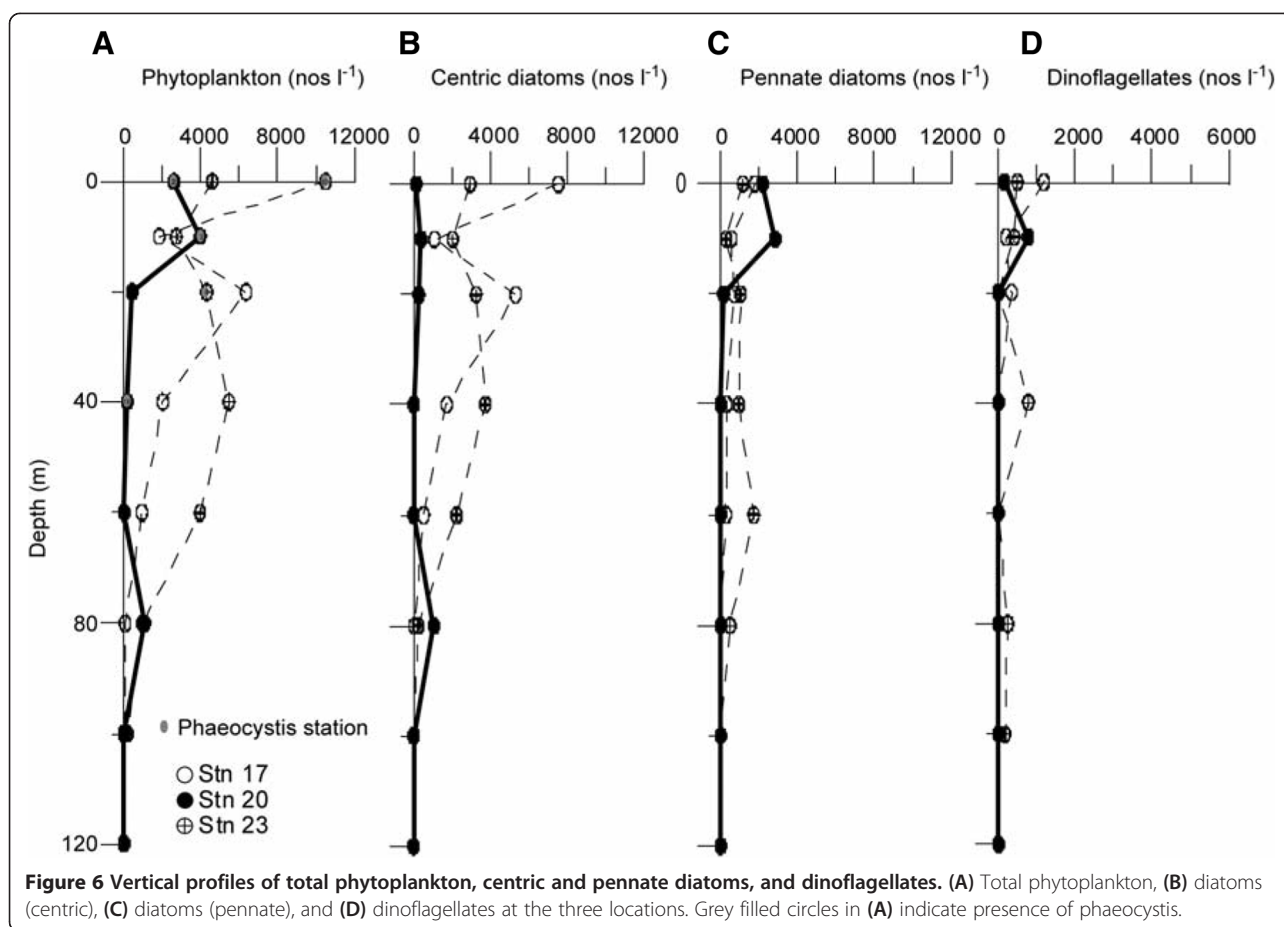
Biochemical composition of pyrosomes

The carbon and nitrogen contents of the pyrosome colonies, expressed as percent of dry weight, were 37.7 and 8.8, respectively. The molar C-to-N ratio, thus works out

to be 5.0. The isotopic values were -19.91‰ for $\delta^{13}\text{C}$ and 7.43‰ for $\delta^{15}\text{N}$. The total protein concentration was approximately 134 mg/g dry wt.

Discussion

Generally, pyrosomes are strong diurnal migrators. During the day, they prefer the safety of the dark mesopelagic zone, while at night they migrate to the surface layer to feed on plankton (Angel 1989; Andersen et al. 1992). In the present study, the longest colony of approximately 2 m long was recovered at night from shallow depths. *P. spinosum* nearly of the same dimension was recovered accidentally with the CTD rosette in the North Atlantic during a cruise of G.O. Sars (see http://www.mar-eco.no/mareco_news/2004/the_pyrosome_story). A much longer (6 \times 0.9 m) colony of *P. spinosum* Herdman was reported from the New Zealand waters (Griffin and Yaldwyn 1970). The occurrence of *P. spinosum* at the surface during midday is possibly due to the presence of a very shallow intense oxygen minimum zone (OMZ), which may act as a physical barrier for vertical movement in the entire North Indian Ocean. Similarly, no clear day-night migration pattern was recorded in *Pyrosoma*



(not identified to the species level) in the open waters (along 88°E) of the Bay of Bengal (Madhupratap et al. 2003), although the *Pyrosoma* colonies there were non tubular, smaller in size (10 × 10 cm), fewer in number, and whitish in color.

As pointed out by Perissinotto et al. (2007), the trophic function, feeding dynamics, as well as ecology and physiology of pyrosomes are not well known. Analysis of gut contents of *Pyrosoma* (Hart, as cited by Culkin and Morris 1970) showed that the main food was phytoplankton (approximately 80%) belonging to the classes Haptophyceae, Chrysophyceae, and Bacillariophyceae, the remainder was composed of protozoan species such as radiolarians and tintinnids. Consistent with this view, Bourguet et al. (2009) found higher values of Chl *a* (38 ± 14.6 ng Chl *a* eq./mg dry weight) in the guts of *P. atlanticum* collected from the NW Mediterranean Sea. The question arises why the *P. spinosum* swarm occurred only at station 20 and not at the other two stations; where the physicochemical conditions were only slightly different? The map of the sea surface height anomaly overlaid with OSCAR

surface current during the study period (Figure 11) depicts offshore advection of waters but no accumulation of water at the swarm site. Thus, one may argue that the swarm of pyrosome was driven by the biological factors. The low abundance of microphytoplankton (as determined by the microscopic counts) at station 20 are indicators of selective feeding of the swarms on the larger plankton-diatoms or that the resultant excretory products (note that the ammonium concentration was higher at the swarm site) might have supported a high population of *Synechococcus* and *Phaeocystis*. On the other hand, it is also possible that the higher abundance of cyanobacteria and flagellates at station 20 (low silica region) as seen from HPLC and flow cytometry data contributed to higher phytoplankton biomass (Chl *a* content). A similar explanation for the occurrence of salps in the northern Arabian Sea has been invoked by Naqvi et al. (2002) who argued that a deficiency of silicate relative to nitrate limits diatom productivity in winter, a period of weak convection-driven vertical mixing. The data obtained in the present study confirm the postulation of Naqvi et al. (2010) that the high nitrate-to-silicate

Table 1 Taxonomic list of phytoplankton (>5 µm) and their abundance at three different stations

Phytoplankton composition	Station 17		Station 20		Station 23
	Cell L ⁻¹ (<100 mt)	Phytoplankton composition	Cell L ⁻¹ (<100 mt)	Phytoplankton composition	Cell L ⁻¹ (<100 mt)
Diatom (centric)					
<i>Bacteriastrium delicatulum</i>	25	<i>Chaetoceros peruvianus</i>	24	<i>Chaetoceros</i> spp.	111
<i>Chaetoceros coarctatus</i> associated with <i>vorticella</i>	42	<i>Corethron hystrix</i>	45	<i>Coscinodiscus</i> spp.	140
<i>Chaetoceros messanensis</i>	85	<i>Fragilaria</i> spp.	152	<i>Fragilaria</i> spp.	75
<i>Chaetoceros peruvianus</i>	25	<i>Rhizosolenia robusta</i>	25	<i>Planktoniella sol</i>	19
<i>Chaetoceros</i> spp.	113	<i>Thalassiosira</i> spp.	89	<i>Pleurosigma</i> spp.	19
<i>Coscinodiscus radiatus</i>	41			<i>Rhizosolenia alata</i>	408
<i>Coscinodiscus eccentricus</i>	2			<i>Rhizosolenia hebetata</i>	152
<i>Coscinodiscus</i> spp.	21			<i>Rhizosolenia imbricata</i>	157
<i>Guinardia flaccida</i>	42			<i>Rhizosolenia robusta</i>	60
<i>Guinardia striata</i>	42			<i>Rhizosolenia shrubsolei</i>	105
<i>Leptocylindrus minimus</i>	190			<i>Rhizosolenia</i> spp.	11
<i>Rhizosolenia alata</i>	404			<i>Rhizosolenia styliformis</i>	494
<i>Rhizosolenia</i> in association with <i>vorticella</i>	98			<i>Thalassiosira</i> spp.	318
<i>Rhizosolenia hebetata</i>	29				
<i>Rhizosolenia imbricata</i>	199				
<i>Rhizosolenia robusta</i>	31				
<i>Rhizosolenia setigera</i>	21				
<i>Rhizosolenia shrubsolei</i>	19				
<i>Rhizosolenia stalterfothii</i>	21				
<i>Rhizosolenia styliformis</i>	521				
<i>Rhizosolenia</i> spp.	21				
<i>Thalassiosira</i> spp.	337				
Diatom (pennate)					
<i>Cocconeis</i> spp.	25	<i>Navicula</i> spp.	43	<i>Coconeis</i> spp.	38
<i>Navicula directa</i>	21	<i>Nitzschia closterium</i>	136	<i>Navicula transitrans f. delicatula</i>	22
<i>Navicula</i> spp.	155	<i>Nitzschia</i> spp.	66	<i>Navicula</i> spp.	49
<i>Navicula transitrans f. delicatula</i>	10	<i>Pseudonitzschia</i> spp.	165	<i>Nitzschia closterium</i>	98
<i>Nitzschia closterium</i>	21	<i>Thalassiothrix</i> spp.	443	<i>Nitzschia</i> spp.	198
<i>Nitzschia</i> spp.	19			<i>Pseudonitzschia</i> spp.	151
<i>Pleurosigma directum</i>	10			<i>Thalassiothrix longissima</i>	241
<i>Pleurosigma</i> spp.	144				
<i>Pseudonitzschia</i> spp.	19				
<i>Thalassiothrix</i> spp.	85				
Dinoflagellates					
<i>Ceratium fusus</i>	21	<i>Amphidinium</i> spp.	21	<i>Amphidinium</i> spp.	19
<i>Ceratium horridum</i>	42	<i>Ceratium fusus</i>	21	<i>Amphisolenia bidentata</i>	46
<i>Ceratium tripos</i>	34	<i>Gymnodium</i> spp.	24	<i>Ceratium tripos</i>	22
<i>Goniodoma</i> spp.	21	<i>Gyrodinium</i> spp.	21	<i>Dinoflagellate cysts</i>	19
<i>Gyrodinium</i> spp.	46	<i>Phalacroma rotundatum</i>	21	<i>Gonyaulax</i> spp.	22
<i>Protoperidinium depressum</i>	42	<i>Prorocentrum dentatum</i>	21	<i>Gymnodium</i> spp.	46
<i>Protoperidinium grande</i>	21	<i>Prorocentrum</i> spp.	21	<i>Gyrodinium</i> spp.	25

Table 1 Taxonomic list of phytoplankton (>5 μm) and their abundance at three different stations (Continued)

<i>Protoperdinium oceanicum</i>	10			<i>Podolampus</i> spp.	11
<i>Protoperdinium steinii</i>	10			<i>Protoperdinium</i> spp.	46
				<i>Pyrophacus horologium</i>	42
Silicoflagellate					
<i>Dictyocha fibula</i>	19	<i>Dictyocha</i> spp.	27		
Chrysophyceae					
<i>Phaeocystis</i> spp.	1,691	<i>Phaeocystis</i> spp.	6,986,667	<i>Phaeocystis</i> spp.	12,285,714
Total cells L ⁻¹	3,103		1,367		3,166

ratio in upwelled waters, promotes the growth of smaller, non diatomaceous phytoplankton as the upwelled water advects offshore. The dominance of *Phaeocystis* in the aged offshore advecting upwelled silica deficient waters in the central Arabian Sea (close to the present study site) has been previously reported by Garrison et al. (1998). Typical succession of phytoplankton community from diatom to *Phaeocystis* appears to be a regular phenomenon in the open waters of the Arabian Sea during late southwest monsoon, which may attract the pelagic tunicates that are able to feed on small particles. Such bloom events are generally triggered by silicate depletion (Batje and Michaelis 1986; Verity et al. 1988) in the euphotic zone. Similar observations were also recorded in the upper 80 m water column at 15°N 64°E under the JGOFS (India) programme (1992 to 1997). At this site, undetectable silicate levels in the upper euphotic zone during southwest monsoon was dominated by *Phaeocystis* bloom (Madhupratap et al. 2000) unlike northeast monsoon where silicate

concentration were relatively higher and largely dominated by diatoms in terms of its diversity (species of *Nitzschia*, *Chaetoceros*, and *Rhizosolenia* were predominant forms) and abundance (Sawant and Madhupratap 1996).

Signatures of the relative dominance of non-diatoms groups were also seen in the HPLC data indicating that nanoflagellates were dominant at subsurface waters of stations 20 and 23 with the characteristic pigment (hexanoxyloxyfucoxanthin) found in the concentration range of 1 to 14 ng/L; its concentration was low (1 to 4 ng/L) at station 17. Further, zeaxanthin, which is a marker pigment of cyanobacteria, also contributed greatly to the total pigment pool (7 ng/L) at station 20. All tunicates are suspension feeders and have the ability to take-up very small particles, including bacteria (Drits et al. 1992, Jørgensen and Goldberg 1953, Harbison and Gilmer 1976, Harbison and McAlister 1979). According to Drits et al. (1992), the minimum size of particles for the pyrosomes to feed should be of considerably <3 μm. Salps,

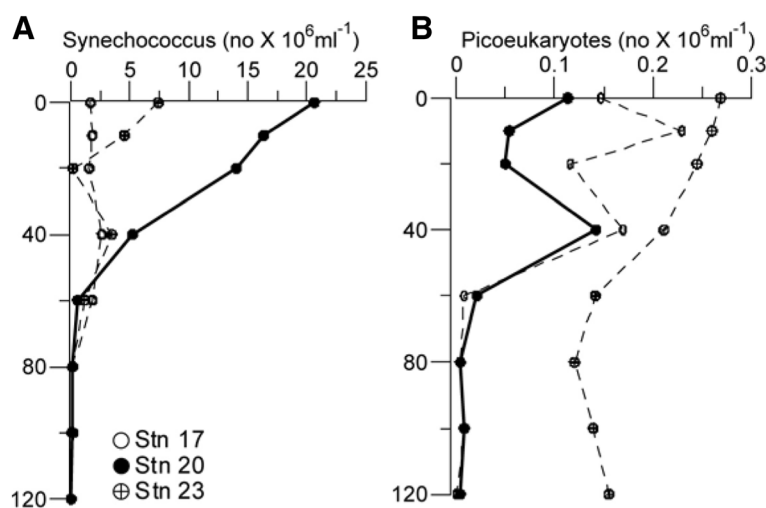


Figure 7 Vertical profiles of *Synechococcus* and picoeukaryotes. (A) *Synechococcus* (×10⁶/ml) and (B) picoeukaryotes (×10⁶/ml) abundance at the three locations.

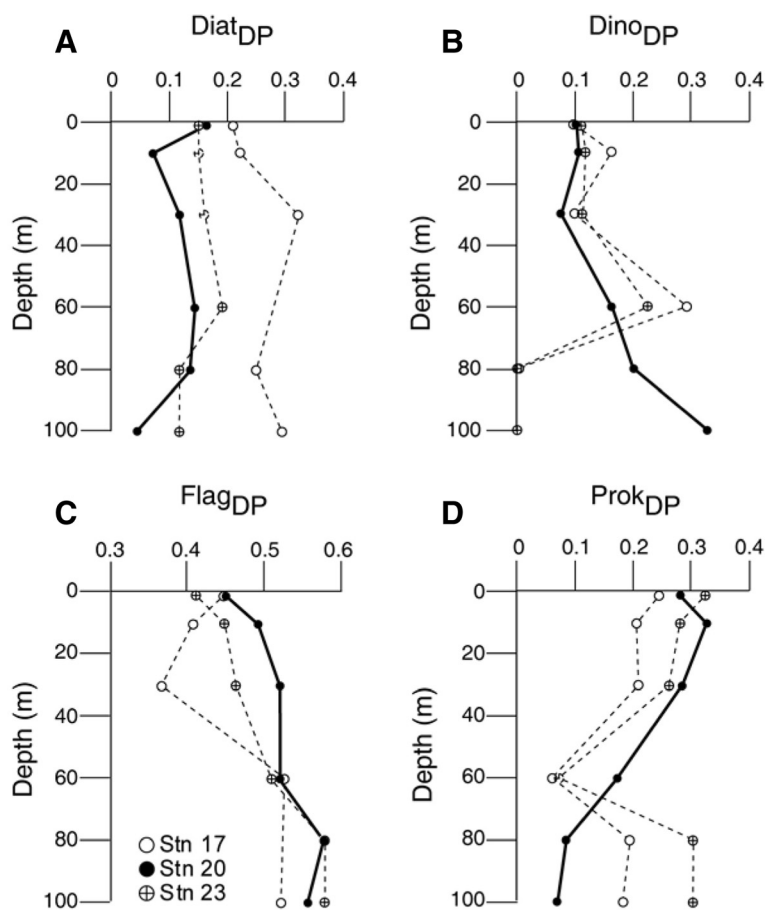


Figure 8 Dominant phytoplankton pigments (A) DiatDP, (B) DinoDP, (C) FlagDP, and (D) ProkDP at three locations.

perhaps the best known of all tunicates, are known to favor low-chlorophyll environments (Harbison et al. 1998) presumably to avoid clogging of their esophagus in high-chlorophyll waters dominated by large phytoplankton such as diatoms. With moderate chlorophyll levels and abundant small-sized autotrophs, we believe conditions prevailing at station 20 were best suited for the proliferation of tunicates in general. Thus, we favor the hypothesis that the pyrosome biomass was sustained by high densities of *Synechococcus* and flagellates that are of the right size (1 to 3 μm) to be retained by tunicates and still not large enough to choke their filtration system.

The high clearance (Harbison and Gilmer 1976, Deibel 1988, Madin and Cetta 1984) and consumption rates make tunicates an important consumer of phytoplankton crop under swarm condition (Drits et al. 1992), due to which these colonial organisms produce very large quantities of faecal pellets and thus play an important role in the flux of organic carbon in the marine ecosystem (Esnal 1999). However, information available on

their ingestion and particle clearance rate, particles/prey, and impact rates on planktonic biomass and production is sparse from the Arabian Sea. The tunicate work in the present study region is mostly restricted to the episodic swarms of salps (Lodh et al. 1998, Nair and Iyer 1974, Godeaux 1972, Naqvi et al. 2002, Ramaswamy et al. 2005). Ramaswamy et al. (2005) suggested that 36% of the PP was exported out of the surface layer largely through the sinking faecal pellets of salps. In the Southern Ocean, ingestion by salps has been reported to account for an even larger fraction (up to 100%) of the PP (Dubischar and Bathmann 1997). Thus, we conclude that at the swarm site (station 20) fate of smaller-sized autotroph biomass was mostly recycling, supporting microbial food web.

Here, we attempted to estimate carbon processing by *P. spinosum* in the Arabian Sea based on the work of Drits et al. (1992) on *P. atlanticum* from off the Congo River mouth, even though these two tunicates are not very similar morphologically. We used the following values: filtration efficiency = 3 to 7.2 $\text{L ind}^{-1} \text{h}^{-1}$;

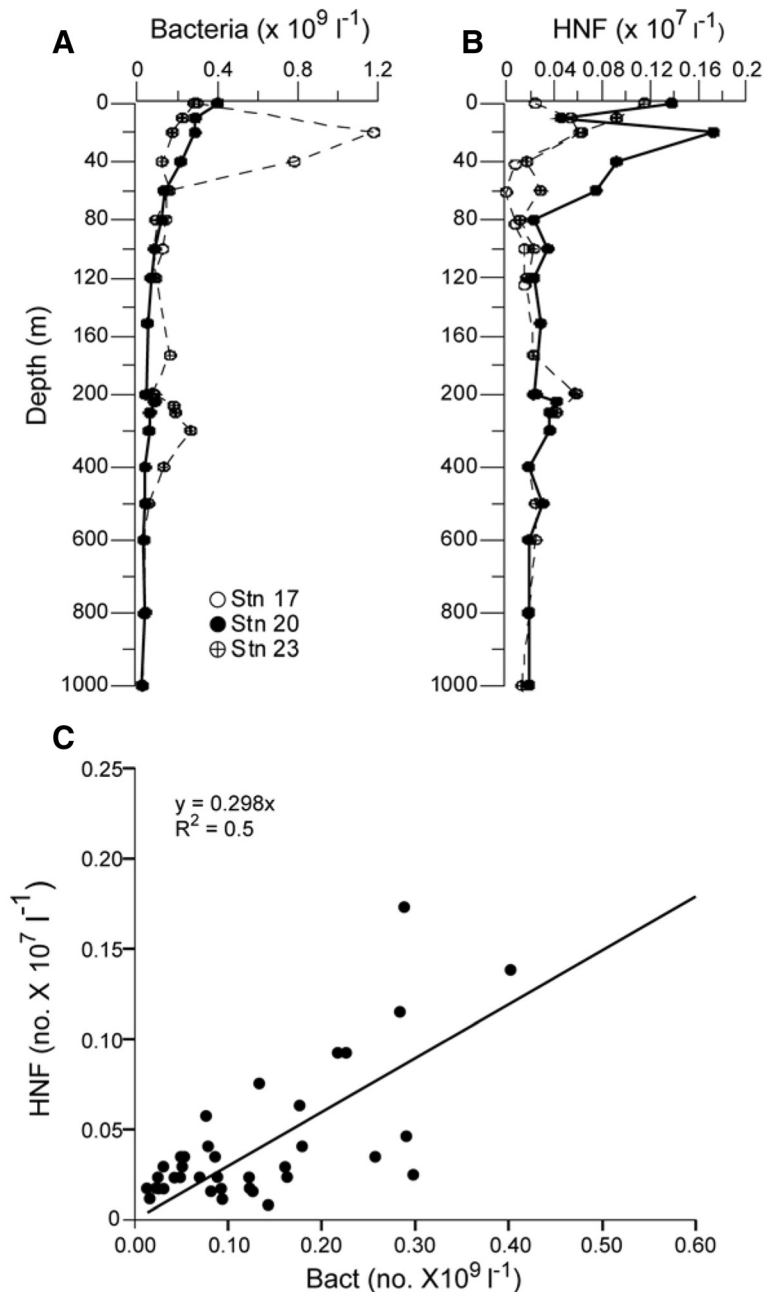


Figure 9 Abundance of (A) bacteria, (B) heterotrophic nanoflagellates at the three locations, and (C) their coupling.

ingestion = 4% to 53% of the phytoplankton standing stock; rate of fecal pellet production = 1.4 to 2.2 pellets h^{-1} zooid $^{-1}$ (this rate is similar to that for salps; Ramaswamy et al. 2005); dry weight of each pellet = 2 μg ; carbon content = 22% of the dry weight, and sinking rate of pellets = 70 m d^{-1} (this is 6 to 12 times slower than that of salps; Ramaswamy et al. 2005). For 24 h, we calculated that a tubular colony having a dimension of 50 \times 150 cm (with 50,000 zooids) would produce 1.7×10^6 to

2.6×10^6 pellets d^{-1} . The amount of water filtered by such a colony would be 3.6 to $8.6 \times 10^6 \text{ L d}^{-1}$. The contribution of such a colony to carbon export from the surface layer would be 0.74 to 1.16 g C d^{-1} . In general, this highlights key role of tunicates in the marine carbon cycle. Readers should use caution when interpreting these estimates. Further, due to the episodic nature of the swarms the significance of pyrosomes to the total carbon export from the surface layer cannot be

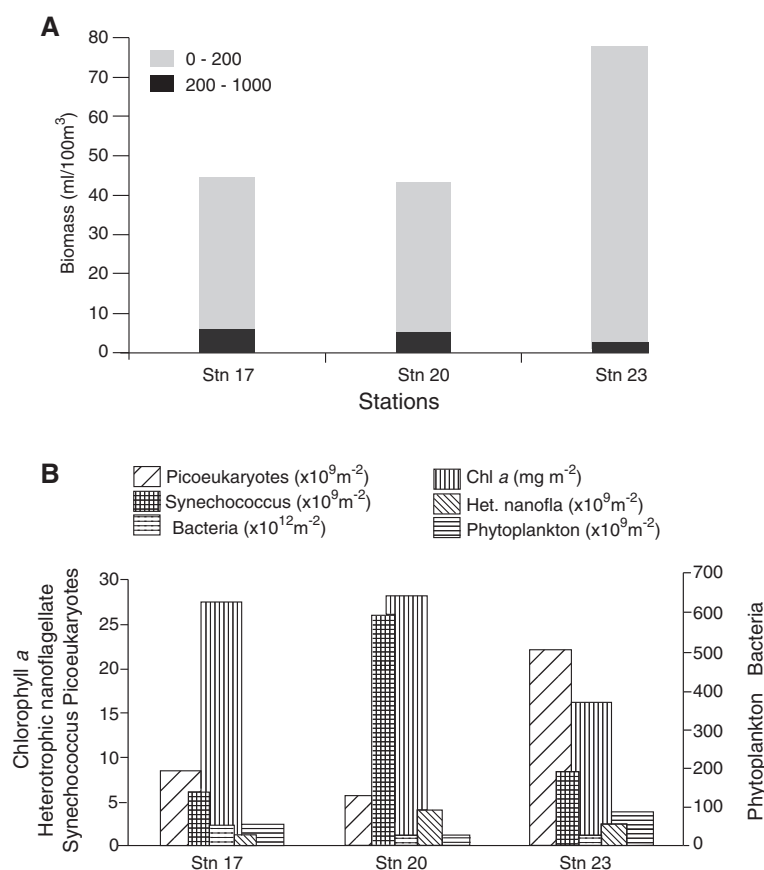


Figure 10 Vertical distribution Mesozooplankton biomass (A) and (B) depth integrated abundance of phytoplankton (>5 μ), het nanoflagellates, het. Bacteria (Bacteria), picoeukaryotes, *Synechococcus*, and chlorophyll *a* concentration (Chl *a*) in upper 100 mt water column at the three different locations.

quantified. In addition to the flux through faecal pellets, sinking of dead colonies is also known to contribute to carbon export. For example, photographs taken at a depth of 5,540 m at the bottom of the Madeira Abyssal Plain showed the arrival of dead *Pyrosoma* on the sea bed, where it was consumed by echinoderms, cnidarians, and arthropods, reflecting the considerable ecological influence of such organisms on the food web in the deep sea (Lampitt et al. 2001).

P. spinosum, similar to *P. atlanticum*, was also found to have a high carbon content (37% of dry weight). The nitrogen content was estimated to be 17% of dry weight. Both carbon and nitrogen contents are higher than reported by Larson (1986) for gelatinous zooplankton including thaliaceans. The molar C-to-N ratio (5) in *P. spinosum* is higher than the value (4) for *P. atlanticum* reported by Gabriel et al. (1988). Yet, this value is lower than the Redfield ratio (6.6), presumably because of the more proteinaceous nature of pyrosomes relative to 'average' marine organic matter. Nonetheless, the protein content of *P. spinosum* obtained by us (134 mg/g) is lower

than the values reported previously (e.g., 355 mg/g; Raymont et al. 1975). Further, the C and N isotopic values of *Pyrosoma* tissue (-19.91% for $\delta^{13}\text{C}$ and 7.43% for $\delta^{15}\text{N}$) are slightly higher than the average marine organic matter. The high carbon and protein contents in their dry weight indicate their potential value as a food source for predators in the ecosystem. Previous work of Harbison (1998), James and Stahl (2000), Childerhouse et al. (2001), and Hedd and Gales (2001) demonstrated that pyrosomes are actually a very important prey item in the diet of many marine mammals, fish, turtle and also albatross, and sea lion.

On the other hand, saphiriniid mysterious parasitic copepods have often been found to be associated with pyrosome colonies (Harbison 1998, Tregouboff and Rose 1957, Monticelli and Lo Bianco 1901, Lindley et al. 2001) including north-western Indian Ocean (Rajaram and Krishnaswamy 1980). In the present study, species of *Sappharina* (*darwinii* and *metallina*) were not found at station 20, but they were present at the other two stations (stations 17 and 23) where the swarm was not found. The absence of these parasitic species at station

Table 2 Taxonomic list of mesozooplankton (>200 µm) and their abundance at three different stations

Mesozooplankton (copepod) composition	0 to 200 mt (org/100 m ³)		
	Station 23	Station 20	Station 17
Calanoida			
Calanidae			
<i>Canthocalanus pauper</i>	*	1	*
<i>Cosmocalanus darwini</i>	1	4	-
<i>Calanoides carinatus</i>		-	1
<i>Undinula vulgaris</i>	2	-	2
<i>Calanus</i> spp.	-	-	1
Eucalanidae			
<i>Eucalanus attenuatus</i>	1	1	1
<i>Eucalanus subcrassus</i>	*		5
<i>Eucalanus</i> spp.	3	3	3
<i>Rhincalanus cornutus</i>	2	*	*
<i>Rhincalanus nasutus</i>	1	-	1
Paracalanidae			
<i>Acrocalanus gibber</i>	5	1	1
<i>Acrocalanus</i> sp.	13	1	*
<i>Paracalanus</i> spp.	20	27	19
<i>Calocalanus pavo</i>	2	-	-
<i>Calocalanus</i> sp.	-	1	*
Euchaetidae			
<i>Euchaeta concinna</i>	-	-	*
<i>Euchaeta wolfendeni</i>	-	-	1
<i>Euchaeta marina</i>	*	-	-
<i>Euchaeta</i> spp.	1	*	1
Scolecithricidae			
<i>Scolecithricella</i> spp.	2	1	1
<i>Scaphocalanus</i> spp.	-	-	1
<i>Scottocalanus helenae</i>	-	-	1
<i>Lophothrix frontalis</i>	-	*	-
Centropagidae			
<i>Centropage furcatus</i>	2	1	1
Temoridae			
<i>Temora stylifera</i>	*	-	1
<i>Temora discaudata</i>	-	-	1
Acartiidae			
<i>Acartia</i> spp.	2	1	2
<i>Acartia erythraea</i>	1	-	1
Clausocalanidae			
<i>Clausocalanus furcatus</i>	1	1	1
Candaciidae			
<i>Candacia pachydactyla</i>	-	-	1

Table 2 Taxonomic list of mesozooplankton (>200 µm) and their abundance at three different stations (Continued)

<i>Candacia curta</i>	1	-	-
<i>Candacia bradyi</i>	*	1	-
Pontellidae			
<i>Labidocera acuta</i>	1	-	-
<i>Labidocera minuta</i>	*	-	-
<i>Labidocera</i> sp.	3	-	1
<i>Calanopia</i> sp.	1	1	-
Aetideidae			
<i>Aetideus</i> sp.	-	*	*
<i>Euchirella amoena</i>	*	*	-
<i>Euchirella maxima</i>	-	*	-
<i>Euaetideus giesbrechti</i>	-	-	*
Augaptiliidae			
<i>Euaugaptilus hecticus</i>	-	-	*
<i>Haloptilus</i> spp.	-	-	*
Heterohabdididae			
<i>Heterohabdus</i> sp.	*	1	1
Lucicutiidae			
<i>Lucicutia flavicornis</i>	2	*	1
<i>Lucicutia ovalis</i>	*	*	1
Mormonillidae			
<i>Mormonilla phasma</i>	*	1	
<i>Mormonilla minor</i>	-	*	1
Metridinidae			
<i>Pleuromamma</i> (juveniles)	-	3	-
<i>Pleuromamma xiphias</i>	-	*	-
<i>Pleuromamma indica</i>	2	-	-
<i>Pleuromamma gracilis</i>	1	*	2
Cyclopoida			
Oithonidae			
<i>Oithona plumifera</i>	2	3	1
<i>Oithona</i> sp.	6	4	3
<i>Oithona helgolandicus</i>	-	1	-
<i>Saphirella tropica</i>	-	*	-
Poecilostomatoida			
Corycaeidae			
<i>Corycaeus catus</i>	1	-	1
<i>Corycaeus</i> sp.	21	6	6
<i>Farranula gracilis</i>	1	-	*
<i>Farranula</i> spp.	5	1	-
Oncaeidae			
<i>Oncaea</i> sp.	26	29	14
Sapphirinidae			

Table 2 Taxonomic list of mesozooplankton (>200 μm) and their abundance at three different stations (Continued)

<i>Sapphirina</i> spp.	-	-	*
<i>Sapphirina gastrica</i>	-	-	1
<i>Sapphirina darwini</i>	*	-	-
<i>Sapphirina metallina</i>	*	-	-
<i>Copilia mirabilis</i>	4	-	*
<i>VetTORIA granulosa</i>	*	-	-
Harpacticoida			
Clytemnestridea			
<i>Clytemnestra scutellata</i>	*	1	1
Euterpinae			
<i>Euterpina acutifrons</i>	1	-	1
Miraciidae			
<i>Macrosetella gracilis</i>	*	-	-
Ectinosomatidae			
<i>Microsetella rosea</i>	-	1	-
<i>Microsetella norvegica</i>	-	-	1
Copepode nauplii	3	3	2
Juvenile copepod	4	-	-

Hyphens indicate that data are absent; *= <100 org/100 m³; 1 = 100 to ≤1,000; 2 = 1,000 to ≤2,000; 3 = 2,000 to 3,000. Numbers 4, 5, 6,... indicate abundances in the range of 3,000 to <4,000; 4,000 to <5,000; 5,000 to <6,000, etc.

20 may be an additional reason for sustaining the prevalence of *P. spinosum* swarm.

Conclusions

During the middle of the day, a pyrosome swarm was observed in the surface waters of the central Arabian Sea. Presence of the perennial oxygen minimum zone at subsurface depth may have restrain pyrosomes from migrating into the deeper layer. Biological factors predominantly seem to have sustained pyrosome swarm. At the swarm site, surface water advected from the coastal upwelling region or entrained from the thermocline characterized by low silicate, and high nitrate and ammonia concentrations perhaps promoted the growth of smaller, non-diatomaceous phytoplankton. Since tunicates have the ability to take-up very small particles, the high densities of *Synechococcus* and flagellates that are of the right size (1 to 3 μm) appear to have offered favorable condition for nourishment of these filter feeders *P. spinosum*. The absence of parasitic species of copepods *Sappharina* (*darwini* and *metallina*) may be an additional reason for sustaining the prevalence of *P. spinosum* swarm. Overall, the occurrence and importance of tunicates such as pyrosomes have been largely overlooked in the northern Indian Ocean and warrant further investigations.

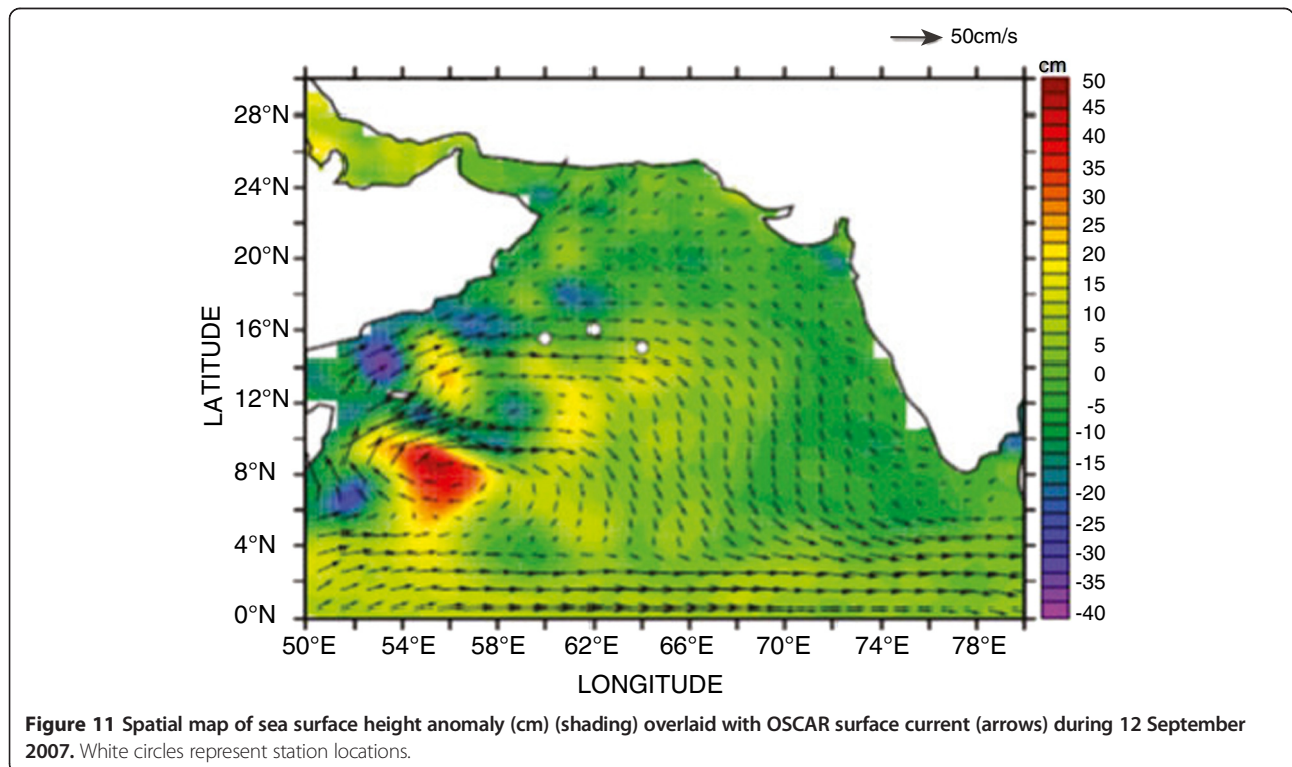


Figure 11 Spatial map of sea surface height anomaly (cm) (shading) overlaid with OSCAR surface current (arrows) during 12 September 2007. White circles represent station locations.

Additional file

Additional file 1: Photograph showing floating *Pyrosoma spinosum* swarms in the surface waters of station 20. (A) Floating colony; (B) colony caught CTD; (C) colony on deck; (D) closer view of colony under microscope; (E) zooids under bright field; and (F) zooids under dark field.

Competing interests

The authors declare that they have no competing interests.

Authors' contributions

MG participated in sample collection and analysis of some of biological parameters and drafted and revised manuscript. SM participated in the cruise and carried out analysis of phytoplankton and zooplankton taxonomy. AP participated in the cruise and carried out chemical measurements. RR participated in the cruise and carried out HPLC-based pigment analyses. SWAN led the cruise, carried out chemical analysis, and helped in drafting and editing of the previous versions of manuscript. All authors read and approved the final manuscript.

Acknowledgements

The authors thank the director of CSIR-NIO for his encouragement in carrying out this study. The authors wish to thank the CSIR (India) for financial support. This work was carried out as a part of network programmes 'CMM0009' and 'NWP 0014'. We thank Mrs. Supriya Karapurkar for elemental/isotopic analyses of samples and Dr. Catherine Sumathi for protein estimation. We are grateful to the captain and crew of R.V. *Roger Revelle* for their help in deck operations and to our colleagues for their assistance in sampling and analysis. This is NIO contribution no. 5684.

Received: 30 May 2014 Accepted: 14 November 2014

Published online: 03 January 2015

References

- Allredge AL (1981) The impact of appendicularian grazing on natural food concentrations *in situ*. *Limnol Oceanogr* 26:247–257
- Andersen V, Sardou J, Nival P (1992) The diel migrations and vertical distributions of zooplankton and micronekton in the Northwestern Mediterranean Sea. 2. Siphonophores, hydromedusae and pyrosomids. *J Plankton Res* 14:1155–1169
- Angel MV (1989) Vertical profiles of pelagic communities in the vicinity of the Azores Front and their implications to deep ocean ecology. *Prog Oceanogr* 22(1):24
- Barlow R, Stuart V, Sessions H, Sathyendranath S, Platt T, Kyewalyanga M, Clementson L, Fukasawa M, Watanabe S, Devred E (2007) Seasonal pigment patterns of surface phytoplankton in the subtropical southern hemisphere. *Deep Sea Res I* 54:1687–1703
- Bary BM (1960) Notes on the ecology, distribution and systematics of pelagic Tunicata from New Zealand. *Pac Sci* 14:101–121
- Bätje M, Michaelis H (1986) *Phaeocystis pouchetii* blooms in the East Frisian coastal waters (German Bight, North Sea). *Mar Biol* 93:21–27
- Booth BC, Lewin J, Postel JR (1993) Temporal variation in the structure of autotrophic and heterotrophic communities in the subarctic pacific. *Prog Oceanogr* 32:57–99
- Bourguet N, Goutx M, Ghiglione J, Pujo-Pay M, Mével G, Momzikoff A, Mousseau L, Guigue C, Garcia N, Raimbault P, Pete R, Oriol L, Lefèvre D (2009) Lipid biomarkers and bacterial lipase activities as indicators of organic matter and bacterial dynamics in contrasted regimes at the DYFAMED site, NW Mediterranean. *Deep Sea Res II* 56:1454–1469
- Bradford MM (1976) A rapid and sensitive method for the quantitation of microgram quantities of protein utilizing the principle of protein-dye binding. *Anal Biochem* 72:248–254
- Brown SL, Landry MR, Barber RT, Campbell L, Garrison DL, Gowing MM (1999) Picophytoplankton dynamics and production in the Arabian Sea during the 1995 Southwest Monsoon. *Deep Sea Res II* 46:1745–1768
- Childerhouse S, Dix B, Gales N (2001) Diet of New Zealand sea lions (*Phocarctos hookeri*) at the Auckland Islands. *Wildl Res* 28:291–298
- Culkin F, Morris RJ (1970) The fatty acids of some cephalopods. *Deep Sea Res* 17:171–174
- Deibel D (1982) Laboratory-measured grazing and ingestion rates of the salp, *Thalia democratica* Forskal, and the doliolid, *Doliolitta gegenbauri* Uljanin (Tunicata, Thaliacea). *J Plankton Res* 4:189–201
- Deibel D (1986) Feeding mechanism and house of the appendicularian *Oikopleura vanhoeffeni*. *Mar Biol* 93:429–437
- Deibel D (1988) Filter feeding by *Oikopleura vanhoeffeni*, grazing impact on suspended particles in cold ocean waters. *Mar Biol* 99:177–187
- Drits AV, Arashkevich EG, Semenova TN (1992) *Pyrosoma atlanticum* (Tunicata, Thaliacea): grazing impact on phytoplankton standing stock and role in organic carbon flux. *J Plankton Res* 14:799–809
- Dubischar CD, Bathmann UV (1997) Grazing impact of copepods and salps on phytoplankton in the Atlantic sector of the Southern Ocean. *Deep Sea Res II* 44:415–433
- Esnal G (1999) Pyrosomatida. In: Boltovskoy D (ed) South Atlantic Zooplankton. Backhuys Publishers, Leiden, pp 1423–1444
- Gabriel G, Dallot S, Sardou J, Fenaux R, Claude C, Isabelle P (1988) C and N composition of some northwestern Mediterranean zooplankton and micronekton species. *J Exp Mar Biol Ecol* 124:133–144
- Garrison DL, Gowing MM, Hughes MP (1998a) Nano- and microplankton assemblages in the northern Arabian Sea during the Southwestern Monsoon, August–September, 1995: a US JGOFS study. *Deep-Sea Res II* 45:2269–2299
- Godeaux J (1972) Pelagic tunicates of the Indian Ocean. *J Mar Biol Ass India* 14:263–292
- Griffin DJG, Yaldwyn JC (1970) Giant colonies of pelagic tunicates (*Pyrosoma spinosum*) from SE Australia and New Zealand. *Nature* 226(5244):464
- Haas LW (1982) Improved epifluorescence microscopy for observing planktonic organisms. *Ann Inst Oceanogr Paris* 58:261–266
- Harbison GR (1998) The parasites and predators of Thaliacea. In: Bone Q (ed) The biology of pelagic tunicates. Oxford University Press, Oxford, pp 187–214
- Harbison GR, Gilmer RW (1976) The feeding rates of the pelagic tunicate, *Pegea confoederata*, and two other salps. *Limnol Oceanogr* 21:517–528
- Harbison GR, McAlister VL (1979) The filter feeding rates and particle retention efficiencies of three species of Cyclosalpa (Tunicata, Thaliacea). *Limnol Oceanogr* 24:875–892
- Hedd A, Gales R (2001) The diet of shy albatrosses (*Thalassarche cauta*) at Albatross Island, Tasmania. *J Zool London* 253:69–90
- Indian Ocean Biological Centre (1973) International Indian Ocean Expedition Plankton Atlas. In: Panikkar NK (ed). UNESCO/NIO, 4(2)
- James JD, Stahl JC (2000) Diet of southern Buller's albatross (*Diomedea bulleri bulleri*) and the importance of fishery discards during chick rearing. *N Z J Mar Freshw Res* 34(3):435–454
- Jørgensen CB, Goldberg ED (1953) Particle filtration in some ascidians and lamellibranchs. *Biol Bull* 105:477–489
- Lampitt RS, Bett BJ, Kiriakoulakis K, Popova EE, Ragueneau O, Vangriesheim A, Wolff GA (2001) Material supply to the abyssal seafloor in the northeast Atlantic. *Prog Oceanogr* 50:27–63
- Larson RJ (1986) Water content, organic content, and carbon and nitrogen composition of medusae from the northeast Pacific. *J Exp Mar Biol Ecol* 99:107–120
- Lindley JA, Hernández F, Scatllar J, Docoito J (2001) *Funchalia* sp. (Crustacea: Penaeidae) associated with *Pyrosoma atlanticum* (Thaliacea: Pyrosomidae) off the Canary Islands. *J Mar Biol Assoc UK* 81:173–174
- Lodh NM, Gajbhiye SN, Nair V (1998) Unusual congregation of salps off Vernal and Bombay. West Coast of India. *J Mar Sci* 17:128–130
- Madhuratap M, Sawant S, Gauns M (2000) First report on a bloom of the marine pyrosomid, *Phaeocystis globosa* from the Arabian Sea. *Oceanol Acta* 23(1):83–90
- Madhuratap M, Gauns M, Ramaiah N, Prasanna Kumar S, Muraleedharan PM, De Sousa SN (2003) Biogeochemistry of the Bay of Bengal: physical, chemical and primary productivity characteristics of the central and western Bay of Bengal during summer monsoon 2001. *Deep-Sea Res II* 50:881–896
- Madin LP (1982) The production, composition and sedimentation of salp fecal pellets in oceanic waters. *Mar Biol* 67:39–45
- Madin LP, Cetta CM (1984) The use of gut fluorescence to estimate grazing by oceanic salps. *J Plankton Res* 6:475–482
- Millar RH (1971) The biology of ascidians. *Adv Mar Biol* 9:1–100
- Monticelli FS, Lo Bianco S (1901) Sullo sviluppo dei peneididel Golfo di Napoli (note riassuntive). *Monit Zool Ital* 11:23–31 (in Italian)
- Morrison JM, Codispoti LA, Smith SL, Wishner K, Flagg K, Gardner WD, Gaurin S, Naqvi SWA, Manghnani V, Prosperie L, Gundersen JS (1999) The oxygen minimum zone in the Arabian Sea during 1995. *Deep-Sea Res II* 46:1903–1931

- Nair VR, Iyer HK (1974) Quantitative distribution of copelates, salps and doliolids (Pelagic tunicates) in Indian Ocean. *Indian J Mar Sci* 3:150–154
- Naqvi SWA, Sarma VSS, Jayakumar DA (2002) Carbon cycling in the northern Arabian Sea during the northeast monsoon: significance of salps. *Mar Ecol Prog Ser* 226:35–44
- Naqvi SWA, Moffett JW, Gauns MU, Narvekar PV, Pratihary AK, Naik H, Shenoy DM, Jayakumar DA, Goepfert TJ, Patra PK, Al-Azri A, Ahmed SI (2010) The Arabian Sea as a high-nutrient, low-chlorophyll region during the late-Southwest Monsoon. *Biogeosciences Discuss* 7:25–53
- Neumann Y (1913) Die pyrosomen und dolioliden der deutschen südpolar-expedition 1901-1903. In: *Ergebn. Deutsche Südpol. Exped Zool* 6:1–34
- Perissinotto R, Mayzaud P, Nichols PD, Labat JP (2007) Grazing by *Pyrosoma atlanticum* (Tunicata, Thaliacea) in the south Indian Ocean. *Mar Ecol Prog Ser* 330:1–11
- Péron F (1804) Mémoire sur le nouveau genre *Pyrosoma*. *Ann Mus Hist Nat Paris* 4(12):437–446
- Rajaram LK, Krishnaswamy S (1980) A note on the similarity in the distribution of Sapphirina (Copepoda, Crustacea) and Salpa (Thaliacea, Tunicata) in the north-western Indian ocean. *Mahasagar - Bull Natl Inst Oceanogr* 13(1):71–77
- Ramaswamy V, Sarin MM, Rengarajan R (2005) Enhanced export of carbon by salps during the northeast monsoon period in the northern Arabian Sea. *Deep-Sea Res II* 52:1922–1929
- Rausch T (1981) The estimation of micro-algal protein content and its meaning to the evaluation of algal biomass. I Comparison of methods for extracting protein. *Hydrobiologia* 78:237–251
- Raymont JEG, Morris RJ, Ferguson CF, Raymont JKB (1975) Variation in the amino-acid composition of lipid-free residues of marine animals from the northeast Atlantic. *J Exp Mar Biol Ecol* 17:261–267
- Roe HSJ, Badcock J, Billett DSM, Chidgey KC, Domanski PA, Ellis CJ, Fasham MJR, Gooday AJ, Hargreaves PMD, Huggett QJ, James PT, Kirkpatrick PA, Lampitt RS, Merrett NR, Muirhead A, Pugh PR, Rice AL, Russell RA, Thurston MH, Tyle PA (1987) Great meteor east: a biological characterisation. Institute of Oceanographic Sciences Deacon Laboratory, Wormley, UK, p 322, Report No. 248
- Roy R, Pratihary A, Gauns M, Naqvi SWA (2006) Spatial variation of phytoplankton pigments along the southwest coast of India. *Estuar Coast Shelf Sci* 69:189–195
- Sawant S, Madhupratap M (1996) Seasonality and composition of phytoplankton in the Arabian Sea. *Curr Sci* 71:869–873
- SCOR (1996) JGOFS report no. 19. Protocols for the Joint Global Ocean Flux Study (JGOFS) core measurements. Scientific Committee on Oceanic Research, International Council of Scientific Unions, Bergen, p 170
- Sewell RBS (1953) The pelagic tunicata. *Brit. Mus. (Nat. Hist.) John Murray Exped.* 1933-34. *Sci Repts* 10:1–90
- Takahashi K, Kuwata A, Sugisaki H, Uchikawa K, Saito H (2009) Downward carbon transport by diel vertical migration of the copepods *Metridia pacifica* and *Metridia okhotensis* in the Oyashio region of the western subarctic Pacific Ocean. *Deep-Sea Res I* 56:1777–1791
- Thompson H (1948) Pelagic tunicates in Australia. Commonwealth Council for Scientific and Industrial Research, Melbourne, p 196
- Tregouboff G, Rose M (1957) Manuel de planctonologie Méditerranéenne, vol II. Centre National de la Recherche Scientifique, Paris
- UNESCO (1994) Protocols for the Joint Global Ocean Flux Study (JGOFS) core measurements. *Man Guides* 29:1–170
- Van Heukelem (2002) HPLC phytoplankton pigments: sampling, laboratory methods, and quality assurance procedures. In: Mueller J, Fargion G (ed) Ocean optics protocols for satellite ocean color sensor validation, Revision 3, vol 2. Goddard Space Flight Center, Greenbelt, USA, pp 258–268. NASA Technical Memorandum 2002–2004
- Van Soest RWM (1981) A monograph of the order Pyrosomatida (Tunicata, Thaliacea). *J Plankton Res* 3(4):603–631
- Vaulot D, Partensky F, Neveux J, Mantoura RFC, Llewellyn C (1990) Winter presence of prochlorophytes in surface waters of the northwestern Mediterranean Sea. *Limnol Oceanogr* 35:1156–1164
- Verity PG, Villareal TA, Smayda TJ (1988) Ecological investigations of blooms of colonial *Phaeocystis pouchetii*. I. Abundance, biochemical composition, and metabolic rates. *J Plankton Res* 10:219–248
- Wiebe PH, Madin LP, Haury LR, Harbison GR, Philbin LM (1979) Diel vertical migration by *Salpa aspera* and its potential for large-scale particulate organic matter transport to the deep sea. *Mar Biol* 53:249–255
- Wishner KF, Gelfman C, Gowing MM, Dawn MO, Mary R, Rebecca LW (2008) Vertical zonation and distributions of calanoid copepods through the lower oxycline of the Arabian Sea oxygen minimum zone. *Prog Oceanogr* 78:163–191

Submit your manuscript to a SpringerOpen® journal and benefit from:

- Convenient online submission
- Rigorous peer review
- Immediate publication on acceptance
- Open access: articles freely available online
- High visibility within the field
- Retaining the copyright to your article

Submit your next manuscript at ► springeropen.com
